









## ARTICLE

# Eyes on the herd: Quantifying ungulate density from satellite, unmanned aerial systems, and GPS collar data

Tabitha A. Graves<sup>1</sup>  | Michael J. Yarnall<sup>2</sup>  | Aaron N. Johnston<sup>2</sup>  |  
 Todd M. Preston<sup>2</sup>  | Geneva W. Chong<sup>3</sup>  | Eric K. Cole<sup>4</sup>  |  
 William M. Janousek<sup>1</sup>  | Paul C. Cross<sup>2</sup> 

<sup>1</sup>U.S. Geological Survey, Northern Rocky Mountain Science Center, West Glacier, Montana, USA

<sup>2</sup>U.S. Geological Survey, Northern Rocky Mountain Science Center, Bozeman, Montana, USA

<sup>3</sup>U.S. Geological Survey, Northern Rocky Mountain Science Center, Jackson, Wyoming, USA

<sup>4</sup>National Elk Refuge, U.S. Fish and Wildlife Service, National Elk Refuge, Jackson, Wyoming, USA

**Correspondence**

Tabitha A. Graves  
 Email: [tgraves@usgs.gov](mailto:tgraves@usgs.gov)

**Present address**

Michael J. Yarnall, Montana Fish, Wildlife, and Parks, Livingston, Montana, USA

**Funding information**

U.S. Fish and Wildlife Service; U.S. Geological Survey

**Handling Editor:** Ryan P. Pavlick

**Abstract**

Novel approaches to quantifying density and distributions could help biologists adaptively manage wildlife populations, particularly if methods are accurate, consistent, cost-effective, rapid, and sensitive to change. Such approaches may also improve research on interactions between density and processes of interest, such as disease transmission across multiple populations. We assess how satellite imagery, unmanned aerial system (UAS) imagery, and Global Positioning System (GPS) collar data vary in characterizing elk density, distribution, and count patterns across times with and without supplemental feeding at the National Elk Refuge (NER) in the US state of Wyoming. We also present the first comparison of satellite imagery data with traditional counts for ungulates in a temperate system. We further evaluate seven different aggregation metrics to identify the most consistent and sensitive metrics for comparing density and distribution across time and populations. All three data sources detected higher densities and aggregation locations of elk during supplemental feeding than non-feeding at the NER. Kernel density estimates (KDEs), KDE polygon areas, and the first quantile of interelk distances detected differences with the highest sensitivity and were most highly correlated across data sources. Both UAS and satellite imagery provide snapshots of density and distribution patterns of most animals in the area at lower cost than GPS collars. While satellite-based counts were lower than traditional counts, aggregation metrics matched those from UAS and GPS data sources when animals appeared in high contrast to the landscape, including brown elk against new snow in open areas. UAS counts of elk were similar to traditional ground-based counts on feed grounds and are the best data source for assessing changes in small spatial extents. Satellite, UAS, or GPS data can provide appropriate data for assessing density and changes in density from adaptive management actions. For the NER, where high elk densities are beneath controlled

Tabitha A. Graves and Michael J. Yarnall are co-lead authors.

This is an open access article under the terms of the [Creative Commons Attribution](https://creativecommons.org/licenses/by/4.0/) License, which permits use, distribution and reproduction in any medium, provided the original work is properly cited.

© 2022 The Authors. *Ecological Applications* published by Wiley Periodicals LLC on behalf of The Ecological Society of America. This article has been contributed to by US Government employees and their work is in the public domain in the USA.

airspace, GPS collar data will be most useful for evaluating how management actions, including changes in the dates of supplemental feeding, influence elk density and aggregation across large spatial extents. Using consistent and sensitive measures of density may improve research on the drivers and effects of density within and across a wide range of species.

#### KEYWORDS

adaptive management, animal aggregation, cervids, chronic wasting disease, contact rates, disease ecology, drone, elk, harvest, imagery, supplemental feeding, winter range

## INTRODUCTION

Wildlife managers need accurate, consistent, and, in some cases, rapid measures of animal density, distribution, and population size to adaptively manage populations. For example, quantifying animal densities in space and time could be used to evaluate whether habitat treatments increase density for a species of conservation concern. Alternatively, for species with disease threats, managers would like density information to inform decisions related to reducing large aggregations that can contribute to high disease prevalence (Descamps et al., 2012; Lloyd-Smith et al., 2005; McCallum et al., 2001; Miguel et al., 2020; Rodríguez-Pastor et al., 2017; Venesky et al., 2011). However, measuring density poses significant challenges because it changes continuously as animals move dynamically across landscapes, making most measurements a snapshot of the distribution for a given time period. Approaches vary in their ability to record this vital information, but the most commonly used approaches summarize density across several weeks to a year. Methods range in complexity and accuracy from indices using raw counts to sophisticated dynamic models (Mills, 2013). Frequently, costs constrain managers to implement basic ground or aerial counts of animals, which, while usually standardized, typically provide minimum counts on a single day for a given area rather than accurate estimates that account for the influence of conditions, observers, and visibility on detection. Nonetheless, these counts, particularly of ungulates, are sufficiently useful for management and state agencies to expend substantial funds to collect these local data to inform harvest strategies.

When more rigorous population estimates are needed, line transect, double observer or repeat observation, and traditional capture–recapture statistical techniques account for detection and estimate population numbers but rarely characterize local spatial variation in density (Borchers et al., 1998; Smyser et al., 2016). Spatial capture–recapture approaches use similar data, also lead to precise estimates, and consider a wide range of local processes, including influences of environmental conditions on habitat selection, density, and connectivity

(Royle, Chandler, Gazenski, et al., 2013; Royle, Chandler, Sollmann, et al., 2013). However, these methods usually reflect average density across long time periods (e.g., a year) and do not yet explicitly measure fine-scale summaries of interest to ecologists, such as local densities or the number and size of groups (Kendall et al., 2019). Alternatively, GPS collars sample animals across time (e.g., Triguero-Ocaña et al., 2019), but little research has evaluated how this subsampling compares with aggregation patterns of entire populations (Sequeira et al., 2019, but see Tosa et al., 2015). Thus, when the goal is to characterize density at fine spatiotemporal scales, we need additional options that are consistent enough for comparisons that are useful for research and management. For example, measurements of density across a season or between years with the locations and timing of hunting seasons could help managers assess options for reducing maximum density (Dougherty et al., 2018; Janousek et al., 2021). For such a purpose, as with the use of minimum counts, approaches that measure densities at specific points in time concurrent with specific management activities or stressors of interest could provide needed information for a number of questions.

For many wildlife species, human activities alter the timing and abundance of food resources, sometimes increasing wildlife aggregations and potential disease transmission (Becker & Hall, 2014; Janousek et al., 2021). The U.S. Fish and Wildlife Service (USFWS) National Elk Refuge (NER) provides supplemental feed to an average of 7500 elk (*Cervus canadensis*) and 500 bison (*Bison bison*) for several months each winter. Feed ground concentration of elk enhanced brucellosis transmission (Cross et al., 2007) and could influence other density-dependent or environmentally transmitted diseases. When chronic wasting disease (CWD), a partially density-dependent disease fatal to deer, elk, and moose, reaches the NER, high elk densities will likely cause high CWD prevalence and subsequent mortality (Galloway et al., 2017). Owing in part to concern over disease transmission, the NER is implementing a plan to reduce feed-season length to reduce densities and potentially disease transmission (USFWS & NPS, 2019). In addition,

managers elsewhere are considering options to reduce aggregations of multiple species to achieve various goals, including decreased pressure on native vegetation in protected areas and depredation of private hayfields. Thus, identifying the best, most rapid, and most cost-effective methods to evaluate how management changes affect ungulate aggregation will be useful for a variety of applications.

Advances in satellite imagery, unmanned aerial system (UAS), and Global Positioning System (GPS) collars have provided new opportunities for estimating animal density (Wang et al., 2019). Enumeration of wildlife using satellite data has proliferated as the spatial and temporal resolution and availability of imagery has increased (Anderson, 2018; Hollings et al., 2018; LaRue et al., 2017). For example, Stapleton et al. (2014) found equivalent detections of polar bears (*Ursus maritimus*) using Worldview 2 satellite (0.5-m resolution) and traditional aerial surveys. However, satellite imagery has not been commonly used to identify ungulates (but see Yang et al. [2014] and Duporge et al. [2020] on elephants) or in temperate regions (Xue et al., 2017). Similarly, UAS data sets allow for a remote assessment of locations and numbers of animals, offer higher resolution, and provide more control over survey timing and conditions (Barasona et al., 2014; Preston et al., 2021). GPS collar technology has also improved, with longer battery life, higher fix rates, and lower spatial error providing finer temporal resolution (Kays et al., 2015).

Researchers in fields as varied as landscape ecology, wildlife ecology, and economics have long recognized the importance of density and developed two families of aggregation metrics to characterize it: area based and distance based. Whereas density inherently depends on area, aggregation can also be described as the relative proximity of individuals, with metrics that do not use area explicitly. For example, disease research evaluates contact frequency and duration (e.g., Cross et al., 2013; Tosa et al., 2017) based on interanimal distances (Kint et al., 2003). Wildlife biologists, focused as much on where animals are as the degree of aggregation, use kernel density estimates (KDEs) to quantify and visualize relative aggregation and consider underlying habitat drivers (e.g., Coe et al., 2018; Johnson et al., 2013). An ideal aggregation metric should be sensitive to density differences, easily interpreted, and consistent across different data sources. These characteristics would enable the detection of the effectiveness of management changes, a description of those changes, and the use of the metric to compare populations across data sources.

Here we provide an integrated assessment of seven aggregation metrics calculated from three concurrently collected data sources (satellite, UAS, and GPS) for their use as an index of density. Specifically, we assess

combinations of data sets and metrics for their use in management decisions and research. We pose the following questions: (1) Which aggregation metrics are most sensitive to changes in aggregation? (2) Are aggregation metrics calculated from different data sources robust enough for comparison across multiple populations? (3) How consistent are animal counts from satellite and UAS images with traditional aerial and ground counts? and (4) Which combinations of data sets and metrics adequately identify changes in aggregation across time periods relevant to management actions? We consider how managers and researchers might decide on an approach for measuring aggregation and illustrate testing for differences in density applied to supplemental feeding. We conclude by suggesting best methods for the NER to measure effects of management changes intended to reduce density and, thus, potentially disease transmission risk.

## METHODS

### Study area

Our study area encompasses ~223 km<sup>2</sup> and is defined by a 2-km buffer around the NER near Jackson, Wyoming, USA (Figure 1). The NER manages wintering elk under the USFWS Bison and Elk Management Plan (USFWS & NPS, 2007) in collaboration with the Wyoming Game and Fish Department (WYGF). The NER initiated a supplemental feeding program in 1912 to mitigate the effects of human land use and development on elk winter range. Start and end dates for the feed season vary annually with snow and forage conditions, but feeding typically occurs daily around 9:00 AM from late January through late March or early April. Managers feed elk in the same four locations each year. The NER is mostly grassland and open shrubland, including sagebrush, with only 6% forested (National Land Cover Database, 2016). The NER neighbors the Bridger-Teton National Forest, the town of Jackson, and Grand Teton National Park, which contains the Jackson Hole airport.

### Data sources

We compared metrics of elk aggregation using three data sources: satellite imagery, UAS imagery, and GPS collar data. We collected data across a range of spatial and temporal scales expected to have varying elk density, specifically targeting data collection to assess variation in aggregation based on seasonal patterns and supplemental feeding. We collected imagery pre-, post-, and during feeding in 1 year, plus during dates typical of feeding in a rare nonfeeding year (Appendix S1: Figures S1 and S2). To



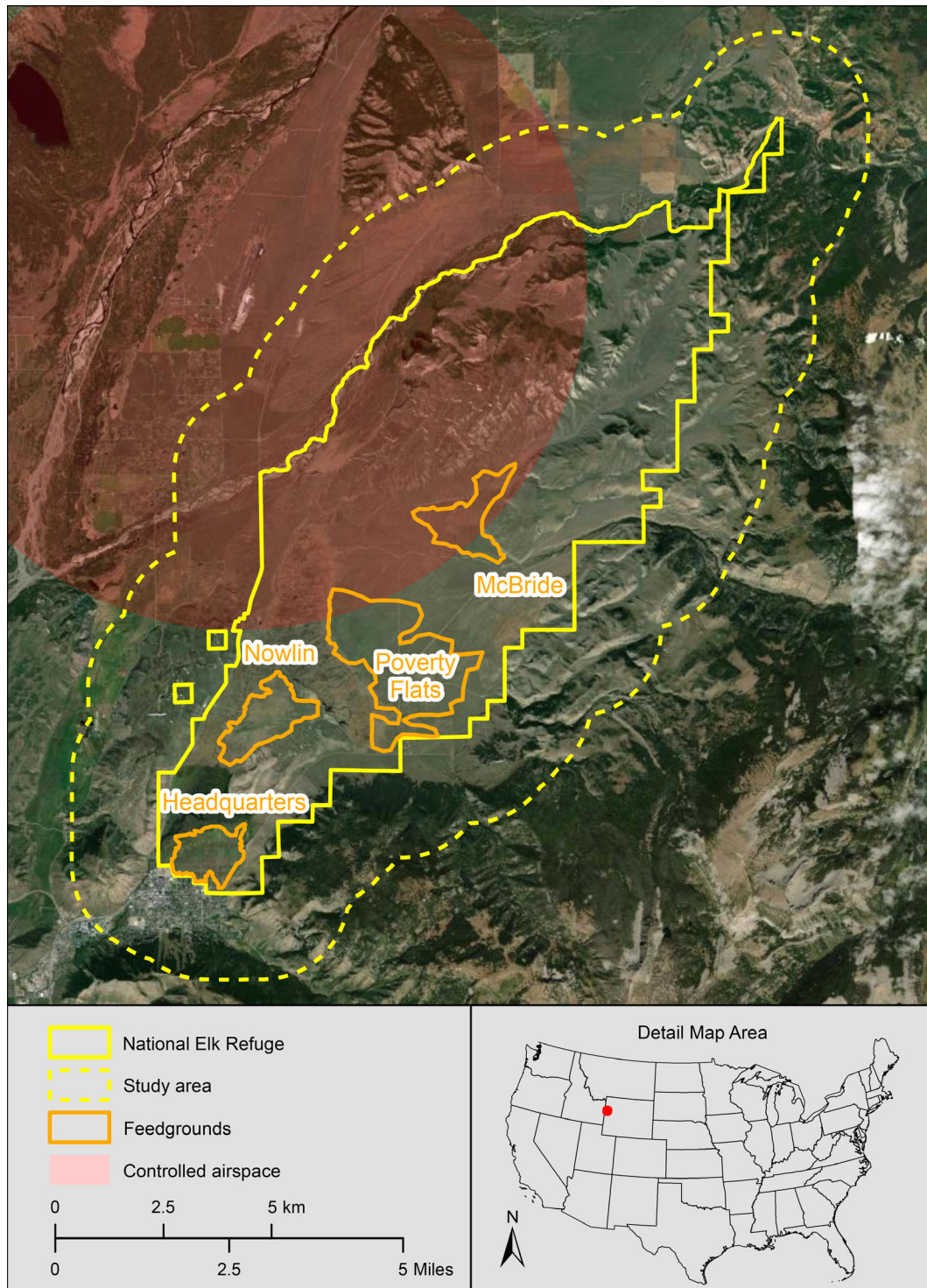


**FIGURE 1** National Elk Refuge in Wyoming, USA

compare metrics across data sources, we quantified elk aggregation at spatial extents matching the smallest extent of the data source in the comparison. We also compared traditional ground and aerial counts with satellite and UAS counts; however, we could not calculate aggregation metrics from these counts because they did not include individual elk locations.

### Satellite imagery

We digitized elk locations using five satellite images obtained from DigitalGlobe (Westminster, Colorado, USA; WorldView-2 satellite, ~0.5-m resolution; WorldView-3 satellite, ~0.3-m resolution) ordered to coincide with UAS flights and two traditional counts (one per

year) (Appendix S1: Table S1). We selected 5 images from the 15 available images based on temporal matching with other data sources, image quality, and resources available to digitize elk in images (Appendix S1: Table S1). Two observers digitized elk locations in pansharpened and orthorectified images using ArcGIS 10.6 (Environmental Systems Research Institute [ESRI]; Redlands, California, USA)—one digitized elk in the 1 February 2019 image and one digitized elk in all other images. Observers initially viewed images at scales of  $\sim 1:2500$  to  $\sim 1:3500$  to identify potential elk and zoomed to scales up to  $\sim 1:600$  for confirmation. To differentiate elk from other features (rocks, shrubs, snow-free patches of ground), observers considered size, color, and shadow of potential elk-like objects. Additionally, observers consulted reference images from other dates to avoid digitizing persistent features across images.

## UASimagery

We acquired images from 24 UAS flights conducted during 4 trips in 2018 and 2019 (Appendix S1: Table S1) using a Solo UAS (3D Robotics, Berkeley, California, USA) equipped with a digital camera (GR model, Ricoh Imaging Co., Tokyo, Japan). We targeted elk herds based on road accessibility for the UAS crew and controlled airspace restrictions from the nearby airport. We built flight plans in the field by triangulating elk aggregations with terrain features visible from both the ground and within Google Satellite images in Mission Planner 1.3.52. The UAS collected still images every second along parallel transects offset by 66 m flying at 150 m altitude at 12 m/s. Respective forelap and sidelap between successive images and transects were 91% and 66% with ground sample distance (image resolution) of 3.9 cm. We conducted most flights 1 h after sunrise, at midday, and 1 h before sunset.

We processed UAS imagery in Agisoft Metashape 1.0.0.1 (Agisoft LLC, St. Petersburg, Russia) and digitized elk locations in ArcGIS 10.6 (Graves et al., 2021). After visually screening photographs for elk, we aligned and georeferenced only those containing animals. The 91% overlap in images helped us align photos with minimal textural features in the snow-covered, relatively flat landscape; however, many photographs contained the same animals. Therefore, we created final orthomosaics for each flight from the minimum number of photographs to produce a complete image. Thus, final orthomosaics included fewer images containing larger scenes (approximately  $194 \times 129$  m), which reduced double counting of animals from movement between successive images. Given the inability to place ground control targets, we rubber-sheeted orthomosaics to National Agricultural

Imagery Program (1 m resolution) imagery before a single observer digitized elk locations. Like the satellite imagery, reference images from other UAS flights helped distinguish elk from landscape features.

## GPScollar and traditional count data

We examined elk location data from 2016 to 2019 for 73 adult female elk fitted with GPS collars on the NER (Telonics TGW-4670-4, Telonics, Inc., Mesa, Arizona, USA). Collars recorded GPS locations every 1.5 h, resulting in  $\leq 16$  daily fixes per elk. We excluded 5 elk with a mean daily fix success rate  $< 0.90$ , leaving 68 elk for analysis. GPS locations represented a small subsample of the population compared to locations derived from satellite imagery but provided higher temporal resolution over a longer duration.

Biologists with WYGF D counted minimum elk numbers annually with a combination of ground-based surveys and helicopter (Bell 47 Soloy) surveys. During aerial classification, biologists photographed large elk herds and counted elk from the photographs later to improve accuracy. In addition, NER staff visually approximated the number of elk in each feed ground (usually rounding to the nearest 100 elk) each day that feeding occurred. We determined that daily observations varied by up to 20% between concurrent observers.

## Aggregation metrics

We considered seven aggregation metrics to quantify how clustered elk were and compared the sensitivity of metrics across data sources (Table 1): interelk distances, nearest-neighbor distances, the cumulative nearest-neighbor distribution, average neighbor distance versus neighbor order, Ripley's K, Lorenz curves, and KDE. The first four metrics are all distance-based measures of aggregation (Wilschut et al., 2015). We compared distributions and summary statistics of aggregation metrics across dates and data sources. We considered two summary statistics for cumulative nearest-neighbor distribution and Ripley's K that describe deviation from complete spatial randomness: the ratio of the area between the expected and estimated curves to the total area under the estimated curve and the ratio of the area under the estimated curve to the area under the expected curve.

We calculated KDEs for each data source and spatial extent to visualize and describe temporal changes in elk density (Calenge, 2006). For each data source and spatial extent, we used the mean bandwidth from the reference method (Calenge, 2006; Gitzen et al., 2006) to estimate KDEs to reduce the influence of bandwidth choice on

**TABLE 1** Aggregation metrics used to characterize elk density and distribution on National Elk Refuge, Wyoming, USA

Metric	Description	Summary statistics	References; R package
Interelk distance distribution	Distribution of all unique pairwise distances between elk	Minimum, first quartile, median, maximum distances	Pebesma (2018); package <i>sf</i>
Nearest-neighbor distance distribution	Distribution of distance from every elk to closest neighbor	Minimum, first quartile median, maximum distances	Dorman (2019); package <i>ngeo</i>
Average neighbor distance	Distance from elk to its nearest, second nearest, ..., farthest neighbor, averaged across all elk locations	Graphical display	Dorman (2019); package <i>ngeo</i>
Cumulative nearest-neighbor distance distribution	Probability of finding nearest neighbor within specified distance	Graphical display, area between observed curve and curve expected under complete spatial randomness	Baddeley et al. (2015); package <i>spatstat</i>
Ripley's K	Expected number of other elk within a given distance of each elk, scaled by intensity	Graphical display, area between observed curve and curve expected under complete spatial randomness	Ripley (1977, 1988), Baddeley et al. (2015); package <i>spatstat</i>
Lorenz curve	Cumulative percentage of elk within given percentage of study area, e.g., most used 5% of cells contain 90% of all elk locations	Graphical display, Gini coefficient	Lorenz (1905), Gini (1912, 1921), Hijmans (2019); package <i>raster</i>
Kernel density estimates (KDEs)	Localized density for overlapping subsets of study area defined by kernel	Graphical display, maximum intensity of elk use, density of elk within utilization polygons, polygon area	Silverman (1986), Worton (1989), Calenge (2006); package <i>adehabitatHR</i>

area estimates across data sets. For satellite and UAS data, we calculated a KDE for each date and flight, respectively. For GPS collar data, after excluding one elk in 2017 and 2019 that wintered outside the study area, we calculated seasonal individual-weighted KDEs from 1 January to 29 April and weekly KDEs centered on satellite dates. From the KDEs we estimated 50%, 70%, and 90% utilization polygons and calculated the corresponding area and density of elk for each polygon.

## Comparisons across data sources

We compared aggregation metrics for three pairs of data sources: satellite–GPS, satellite–UAS, and UAS–GPS. We considered two spatial extents—the full study area (satellite–GPS) and the UAS extents (UAS–satellite, UAS–GPS). For satellite–GPS and UAS–GPS comparisons, we selected each elk's GPS fix nearest in time to the satellite image (range: 18–43 min) or UAS flight midpoint (range: 1–42 min). For some UAS flights, few GPS locations were within the spatial extent of the UAS imagery. Therefore, we report only UAS–GPS comparisons with at least 9 collared elk, equivalent to 36 pairwise comparisons. We used Pearson correlations to assess how aggregation summary statistics compared across data sources. To evaluate the sensitivity of metrics to

changes in aggregation, we calculated the coefficient of variation (CV) for summary statistics of each metric for each data source. We assessed the distribution of the CVs across metrics using a k-means cluster analysis to determine metric sensitivity to changes in aggregation.

Traditional classification counts included locations for elk groups outside feed grounds, and ground counts consisted of total counts by feed ground. We grouped elk in satellite imagery by feed ground and compared the total number of elk marked in satellite imagery to ground or helicopter counts. The time between satellite images and traditional counts ranged from zero to 2 days; although some elk moved between counts, we considered this reasonable based on available data and size of the survey area (~223 km<sup>2</sup>) (Janousek et al., 2021). We conducted all analyses in the statistical computing environment R, version 3.5.3 (R Core Team, 2019).

## Evaluation of supplemental feeding on aggregation

We quantified mean differences in density during fed versus unfed times using metrics sensitive to changes in elk distribution (CV > 0.4). For satellite and GPS data, we tested significant differences in aggregation for 4 days (two



fed, two unfed) with two-sample *t*-tests ( $\alpha = 0.05$ ). For UAS data, we used a linear model with mixed effects from the R package *lme4* (Bates et al., 2015) to evaluate within-day changes in aggregation using the log of density as the response variable. We used only 2019 UAS flight data, which targeted one elk group each day, providing 2 days of replication for before, during, and after feeding. We included random intercepts for each day to account for differences in elk groups across days and allow analysis of repeated measures. We combined pre- and postfeeding as unfed because aggregation was similar during these times. We tested the significance of time of day and effect of feeding with Type II Wald *F*-tests with the Kenward–Roger estimate for degrees of freedom (Kenward & Roger, 1997) in the R package *car* (Fox & Weisberg, 2011) and reported differences in factor levels from Wald *z*-tests.

## RESULTS

### Aggregation metrics compared across data sources

Correlations of summary statistics for matching spatial and temporal extents across satellite, UAS, and GPS

collar data were large ( $>0.67$ ) and positive for KDE density and polygon area, first quartile and median interelk distance, cumulative nearest-neighbor distribution, Ripley’s K summaries, and the Gini coefficient but were smaller for maximum interelk distance and median and maximum nearest-neighbor distances (Table 2). Some of the highest consistent correlations were for the KDE polygon area, with the correlations between satellite–GPS and satellite–UAS comparisons all over 0.95, indicating that for the same spatial extent and approximate time, if the satellite-derived KDE polygon area was small, the GPS-derived or UAS-derived KDE polygon areas were also small. Graphical comparisons of interelk distance distributions showed similar aggregation patterns across data sources (Figure 2), and KDEs identified similar locations of concentrated use (Figure 3). UAS aggregation metric patterns matched those from GPS and satellite data sources well even in one case where timing differences and resulting animal movement led to substantially different numbers of elk (26 March 2019) (Figure 2b). We excluded the postfeeding satellite image (19 April 2019) from satellite–GPS comparisons because patchy snow conditions limited visibility of elk in parts of the image (but not where UAS flights occurred) (Appendix S1: Figures S1a,d and S3a,b).

**TABLE 2** Correlations across matched spatial and temporal extents for summary statistics of aggregation metrics calculated from satellite, global positioning system (GPS) collar, and unmanned aerial system (UAS) derived elk locations on National Elk Refuge, Wyoming, USA. We did not calculate the correlation for kernel density estimate (KDE) density because GPS data used a full week of locations for each elk, complicating interpretation. NN = nearest neighbor

Metric	Satellite–GPS correlation ( <i>n</i> = 4)	Satellite–UAS correlation ( <i>n</i> = 4)	UAS–GPS correlation ( <i>n</i> = 7)
Elk density inside 50% KDE polygon	NA	0.674	NA
Elk density inside 70% KDE polygon	NA	0.979	NA
Elk density inside 90% KDE polygon	NA	0.972	NA
50% KDE polygon area	0.953	0.972	NA
70% KDE polygon area	0.992	0.981	NA
90% KDE polygon area	0.983	0.995	NA
First quartile interelk distance	0.768	0.995	0.967
Median interelk distance	0.784	0.978	0.813
Maximum interelk distance	0.611	0.963	0.902
Median NN distance	0.511	−0.314	0.671
Maximum NN distance	0.424	0.599	0.497
Cumulative NN estimated area/theoretical area	0.858	0.848	NA
Cumulative NN area between/estimated area	0.855	0.847	NA
Ripley’s K estimated area/theoretical area	0.972	0.746	NA
Ripley’s K area between/estimated area	0.977	0.769	NA
Gini coefficient	0.821	0.974	0.820

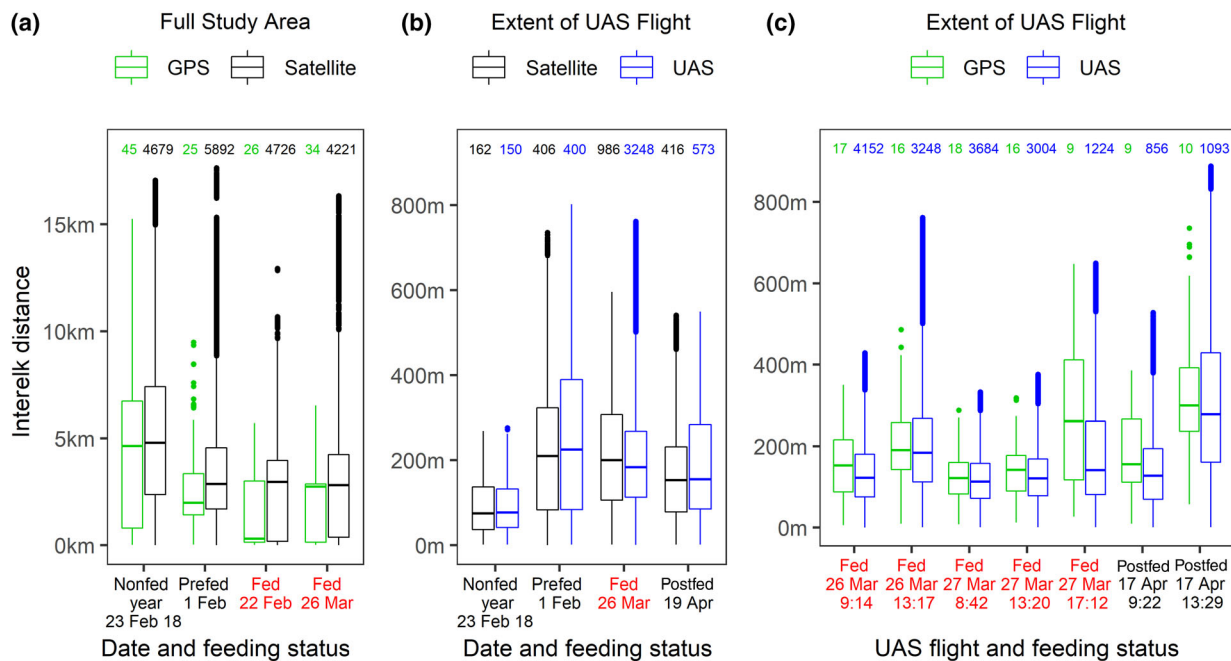


**FIGURE 2** Interelk distance distributions for matching spatial extents of (a) satellite–Global positioning system (GPS) (full study area), (b) satellite–unmanned aerial system (UAS) (flight extent), and (c) GPS–UAS (flight extent, dates with  $n \geq 9$  elk,  $\geq 36$  pairs) data on the National Elk Refuge, Wyoming, USA. Each box contains the first through third quartiles with a horizontal midline for the median and whiskers for the interquartile range\*1.5. Sample size of elk indicated at top of plot (2019 unless otherwise indicated)

## Sensitivity of metrics to changes in aggregation

KDE-based metrics (density and polygon area) and first quartile interelk distance had the greatest variation (i.e., the highest CV) among metrics and, thus, the greatest sensitivity to changes in aggregation (Table 3). Other metric summary statistics (median and maximum interelk distance, median and maximum nearest-neighbor distance, cumulative nearest-neighbor distribution, Ripley's K, and Gini coefficient) exhibited lower CVs or had CVs that were inconsistent across data sources. The k-means cluster analysis ( $k = 2$ ) suggested a natural break between highly sensitive and less sensitive metrics at  $CV = 0.4$ .

## Satellite and UAS compared to traditional survey methods

We compared satellite elk counts to two traditional classification counts (an annual minimum count composed of helicopter and intensive ground counts) and two feed-ground counts (less intensive surveys conducted while feeding). Two UAS flights coincided with feed-ground counts and counts differed by approximately 1% and 12% (26 and 27 March 2019, respectively). However, satellite-

derived counts were always lower than classification and feed-ground counts (Appendix S1: Table S2).

## Effects of supplemental feeding on aggregation

Higher aggregation during supplemental feeding versus nonfeeding was evident ( $p < 0.05$ ) (Table 4) for most aggregation metrics that were sensitive to changes in elk distribution ( $CV > 0.4$ ) across data sources. Metrics based on KDEs consistently identified higher aggregation during feeding across data sources. For example, elk densities within 50% KDEs estimated from satellite imagery ranged 1.33 to 3.34 times higher on fed versus unfed dates (Figures 3a, c). The areas within those 50% utilization polygons ranged from 1.85 to 2.94 times smaller on fed versus unfed dates. Similarly, GPS-derived 50% utilization polygons were 1.39 to 4.76 times smaller during fed versus unfed weeks (Figure 2b,d), and maximum intensity of use was 1.63 times larger in 2017 and 2.71 times higher in 2019 compared to 2018 (unfed) (Appendix S1: Figure S3). In UAS imagery, analysis provided strong evidence ( $F_{1,4} > 38$ ,  $p \leq 0.003$ ) of feeding effects based on elk densities within utilization polygons. The UAS data also showed that aggregation was similar



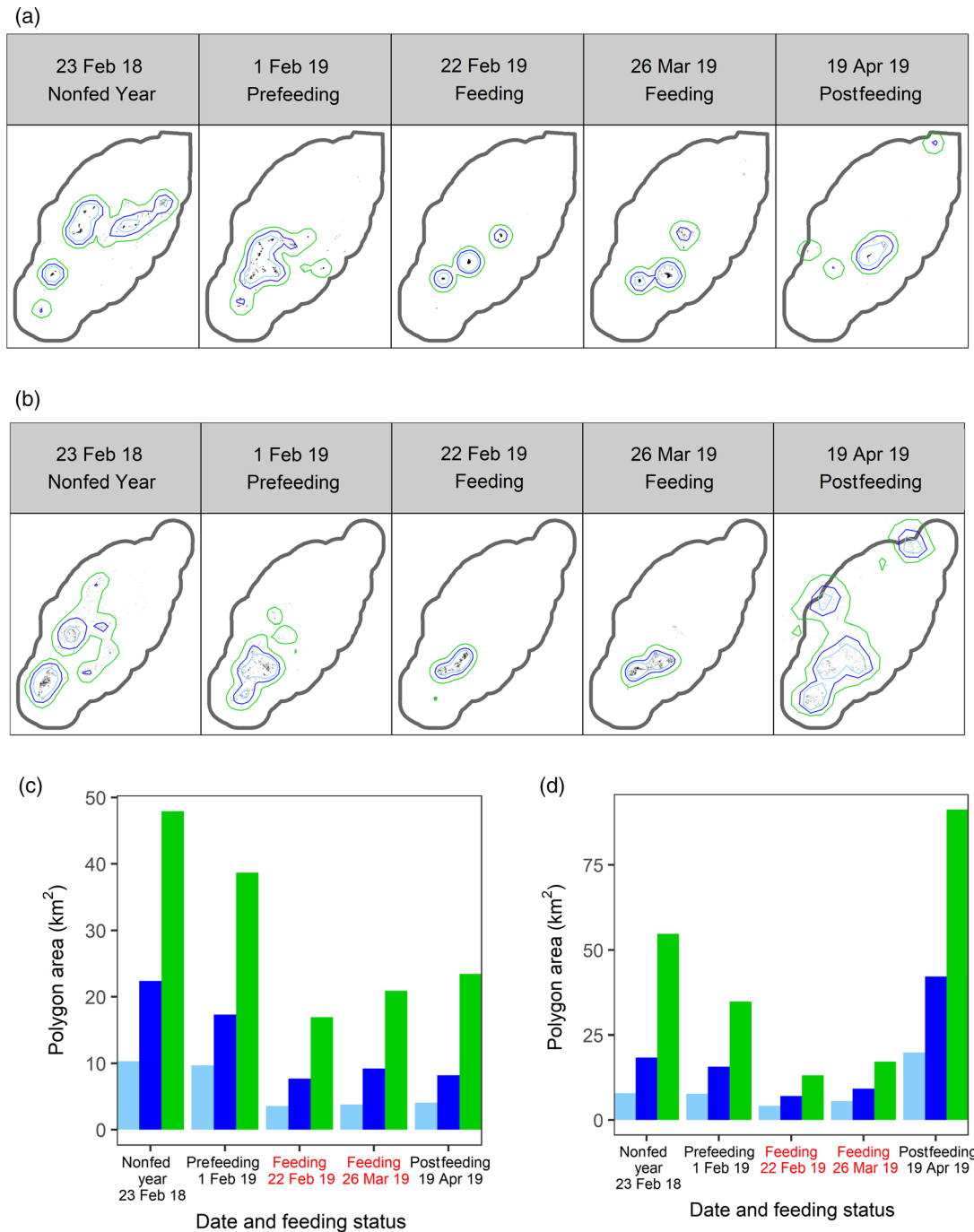


**FIGURE 3** Elk locations (black dots) shown with 50 (light blue), 70 (blue), and 90 (green) percentage utilization polygons on the National Elk Refuge, Wyoming, USA (black polygon shows study area outline) for (a) satellite locations and (b) weekly global positioning system (GPS) locations, and summaries of utilization polygon area for (c) satellite locations and (d) GPS locations. Note reduced satellite-derived utilization polygon size on 19 April 2019 from poor image quality

during the morning and midday flights but decreased in the evening ( $z \geq 2.26, p \leq 0.024$ ).

Calculated elk densities depended on the scale of the utilization polygon. For example, satellite-derived elk densities inside 50% utilization polygons ranged from 839 to 1089 elk/km<sup>2</sup> for fed versus 158 to 437 elk/km<sup>2</sup> for unfed dates, while densities inside 90% utilization polygons ranged from 198 to

274 elk/km<sup>2</sup> for fed versus 38 to 149 elk/km<sup>2</sup> for unfed dates.

### DISCUSSION

Our results suggest that all three data sources (satellite, UAS, and GPS) can be used individually in adaptive

**TABLE 3** Coefficients of variation (CV) for summary statistics of aggregation metrics calculated from satellite, global positioning system (GPS) collar, and unmanned aerial system (UAS) derived elk locations in National Elk Refuge, Wyoming, USA

Metric	Satellite CV	UAS CV <sup>a</sup>	GPS CV <sup>b</sup>
Elk density inside 50% KDE polygon	0.523	1.104	NA
Elk density inside 70% KDE polygon	0.496	1.222	NA
Elk density inside 90% KDE polygon	0.424	1.370	NA
50% KDE polygon area	0.537	0.473	0.691
70% KDE polygon area	0.489	0.513	0.758
90% KDE polygon area	0.472	0.534	0.757
First quartile interelk distance	0.922	0.402	1.20
Median interelk distance	0.285	0.422	0.742
Median NN distance	0.177	0.461	0.668
Cumulative NN estimated area/theoretical area	0.004	0.034	0.015
Cumulative NN area between/estimated area	0.011	0.191	0.050
Ripley's K estimated area/theoretical area	0.289	0.529	0.410
Ripley's K area between/estimated area	0.102	0.289	0.182
Gini coefficient	0.006	0.082	0.001

Abbreviations: KDE, kernel density estimate; NN, nearest neighbor.

<sup>a</sup>Calculated using all 24 flights, with extent for each flight set to flight extent.

<sup>b</sup>Using dates corresponding to satellite images. Because we used a full week for each elk and thus have duplicate locations for each elk, it is incorrect to interpret density here.

**TABLE 4** Mean differences in aggregation ( $\Delta$ ,  $SE$ ) during times of supplemental feeding relative to nonfeeding based on satellite and global positioning system (GPS) ( $n = 2$  fed, 2 unfed in 2018 and 2019) locations and median change in log (density) ( $ML\Delta$ ,  $SE$ ) for unmanned aerial systems (UASs;  $n = 6$  fed, 12 unfed observations over 6 days with 3 flights/day in 2019) in National Elk Refuge, Wyoming, USA. Note that units differ based on analysis method

Metric	Satellite		UAS <sup>a</sup>		GPS <sup>b</sup>	
	$\Delta$	$SE$	$ML\Delta$	$SE$	$\Delta$	$SE$
Elk/km <sup>2</sup> inside 50% KDE polygon	580**	136	1.50***	0.24	10.9*	NA
Elk/km <sup>2</sup> inside 70% KDE polygon	278*	106	1.73***	0.22	7.94**	NA
Elk/km <sup>2</sup> inside 90% KDE polygon	114*	46.1	1.97***	0.27	4.78**	NA
50% KDE polygon area (km <sup>2</sup> )	-6.33***	0.34	-0.0005	0.005	-2.90**	0.71
70% KDE polygon area (km <sup>2</sup> )	-11.4**	2.6	-0.015	0.012	-8.88**	1.72
90% KDE polygon area (km <sup>2</sup> )	-24.4**	5	-0.045	0.024	-29.6**	10.2
First quartile interelk distance (m)	-1769**	351	-35.0*	14.1	-966**	312

\* $p < 0.1$  \*\* $p < 0.05$ , \*\*\* $p < 0.01$ ;  $p$ -values for satellite and GPS are one-sided.

<sup>a</sup>Exponentiated effect sizes are 4.48 (50% KDE), 5.64 (70% KDE), and 7.17 (90% KDE) times higher than median density without feeding.

<sup>b</sup>Kernel densities from GPS-collared elk for a full week, scaled by number of collared elk.

management frameworks to evaluate changes in aggregation over time for a focal population if biologists collect data under consistent field conditions. All data sources concurred that elk aggregations were higher during supplemental feeding and tracked changes associated with feeding. KDE-based metrics and the first quartile of interelk distances best tracked and were most sensitive to large differences in aggregation across data sources. The kernel density approach simultaneously yielded information about the

location of aggregations, which may be useful for the management of environmentally transmitted diseases.

## Satellite

Despite some challenges, satellite imagery successfully detected changes in elk aggregation across periods with and without supplemental feeding on the NER. We relied

on photo interpretation in this temperate landscape to identify elk because elk shared spectral characteristics with landscape features, which prevented the use of automated detection methods (LaRue et al., 2015). We confidently identified most elk in imagery but had difficulty discriminating elk under some conditions (e.g., patchy snow so animals blended with background, cloud cover, distortion in the image, low lighting). Thus, high-resolution satellite imagery can provide useful data in some temperate-region habitats and may be appropriate for interannual comparisons under similar conditions, particularly given a priori knowledge of species behavior and occurrence within the focal area. However, detection rates have the potential to vary under heterogeneous land, cloud, and snow cover, and further research on the role of detection on aggregation metrics may be needed for some uses of this data source.

### Unmanned aerial systems

UAS also identified differences in aggregation patterns resulting from supplemental feeding. Because elk are very clearly visible in UAS imagery and being overhead meant a clear view of all elk in an area, the detection rate of elk most likely approached 1 in the areas surveyed (Figure 4). However, much of the NER is below controlled airspace, and we could not fly all feed grounds.

Flight altitude restrictions also limited our ability to cover larger areas. UAS may be most useful in areas where flights can cover the full wintering grounds and in comparisons of changes at fine spatial scales. For example, UAS would be most appropriate at the NER for evaluating the effects of varying feeding drop rate, line spacing, or area. Recent and future advances in UAS technology (e.g., longer flight duration, larger payload capacities, and multiple sensor packages—combined thermal and visual imagery) (Witczuk et al., 2017) will improve the utility of UASs for adaptive management.

### Global Positioning System

Our results suggest that GPS collars provide the best data for large extents when the focus is on temporal variation. On the NER, methods of deploying collars were consistent across years of study. However, differences in the approach to capturing animals or opportunistic collaring of animals with different movement patterns could limit interannual comparisons of aggregation using GPS data in other areas. Also, because all GPS-collared elk in this study were female, results reflect only female or potentially mixed-sex groups. Standardizing the approach to collaring, maintaining large numbers of collars, recollaring the same animals, collaring males, and examining the data for changes in collar deployment locations

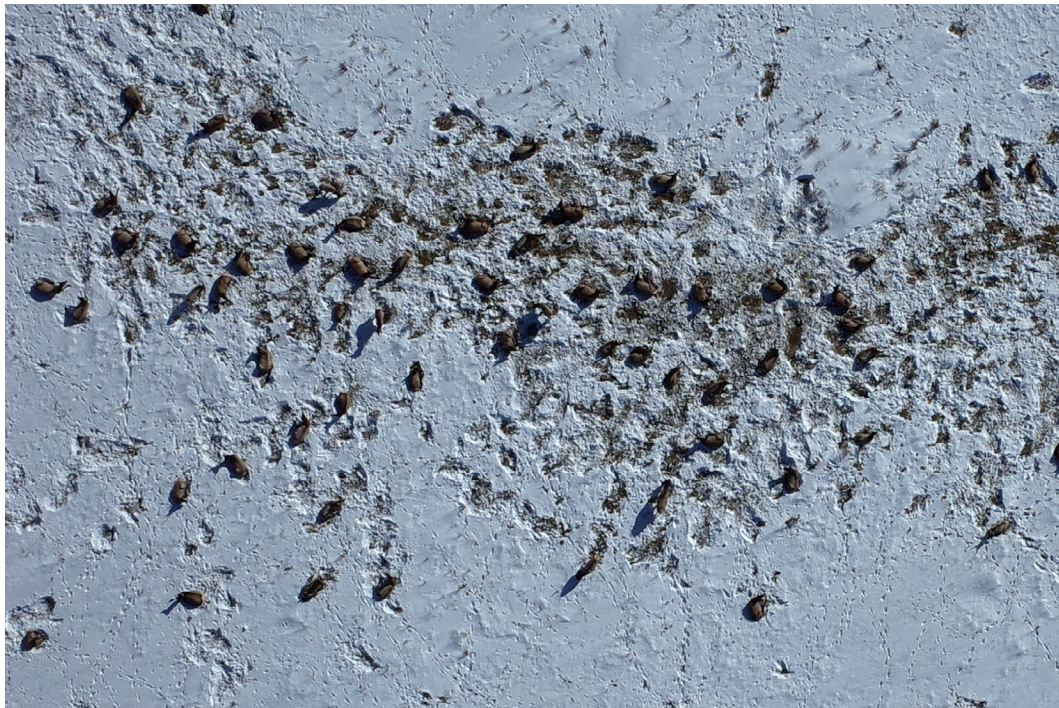


**FIGURE 4** Unmanned aerial system image with patches of melted snow in elk bedding area from 31 January 2019 illustrating that elk can typically be distinguished even in cases where prior bedding locations are a color similar to that of elk



and herd associations could improve the utility of GPS collar data in aggregation comparisons.

## Comparisons across data sources

Our analyses suggest that comparing aggregation across data sources can be useful but requires consideration of spatial and temporal scale as well as data source quality. For example, elk moved outside the small spatial extent of one satellite–UAS comparison in 40 min, producing different counts but similar aggregation measures, because the UAS data were still representative (26 March) (Figure 2). When comparing aggregation across data sources, researchers should consider whether potential biases within each data source were minimized (e.g., using known peak aggregation times to minimize the effects of fine-scale temporal variation). We highlighted a date when poor conditions for identification of elk with satellite imagery affected densities and summary statistics, which led us to exclude these data from further analysis (Appendix S1: Figure S1). Before using summary statistics of aggregation metrics, screening for the obfuscation of important patterns will provide insight for interpretation and use. For example, the median interelk distance can be misleading when subgroups of animals occur, and the full interelk distribution is multimodal (Appendix S1: Figure S3). We did not fit predictive models to translate densities across data sources because of limited sample sizes for comparisons (four for satellite–GPS and satellite–UAS, seven for GPS–UAS comparisons), but this step would facilitate comparisons of aggregation across multiple data sources.

## Data choice

Assessing what data source to use for research or adaptive management requires careful consideration of project goals, study area conditions, and available resources. Satellite imagery can be the least expensive when adequate resolution images are free, requiring only a few hours to order and 1–2 days to digitize elk in a NER-sized (~223 km<sup>2</sup>) image, but it requires consistent conditions and consistency in photo interpretation for useful comparisons. We requested multiple consecutive days of Worldview-2 or 3 imagery during good weather windows, which resulted in approximately one useful (though not always ideal) image per request. Although the Worldview-3 images had higher spatial resolution than Worldview-2 images, weather and contrast conditions had greater effects on the utility of an image for detecting elk versus image sources. UASs provide higher-resolution

images than satellites, are not obstructed by cloud cover, and can be quickly scheduled to accommodate good weather conditions (Appendix S1: Figure S2). Our quadcopter, which had a limited flight time and range (12 min and ~1 km, respectively), was most suitable for targeted flights over smaller areas. Other UASs, such as fixed-wing models or longer-duration rotorcraft, can cover much larger areas per flight. The most expensive option, GPS collars, can address fine-scale temporal variation when distributed well but typically require handling relatively large numbers of animals collared within a wintering range or other high-density area (Cross et al., 2012). Detection of contacts and accurate measurement of other metrics will be highest if fix rates are high and GPS location error is small, which occurred in this study. Data obtained during capture (e.g., samples for disease, body condition), and the ability to use location data to quantify contact rates (Janousek et al., 2021) and answer other habitat use and migration questions, may justify the cost (e.g., Mikle et al. 2019).

Because of controlled airspace restrictions over the NER, neighboring forested areas, and plans on reducing feeding during springtime when elk are harder to identify in satellite imagery, we expect continued GPS collar data will best allow evaluation of the effects of planned adaptive management on aggregation at the NER. Combining GPS collar data collection with traditional classification counts will provide continued information on how the GPS collar sample relates to the spatial distribution of the full wintering population during periods of maximum density. Targeted UAS flights would best quantify changes in aggregation from fine-scale alterations in feeding operations outside controlled airspace.

## CONCLUSIONS

All data sources indicated that elk densities were substantially higher during feeding. Elk identified in the two satellite images when feeding occurred, both likely undercounts, produced elk densities within 50% KDE polygons of 839 and 1089 elk/km<sup>2</sup> (Figure 3a) (22 February 2019 and 26 March 2019). These densities are much greater than the 16–100 elk/km<sup>2</sup> in Rocky Mountain National Park, which had a 13% CWD prevalence (Monello et al., 2014). The relationship between CWD and host-density is unresolved (Potapov et al., 2016; Storm et al., 2013) but probably depends on the spatial scale of the analysis and how local group sizes scale with population size (Cross et al., 2009). However, denser concentrations of elk on the NER are likely to translate into higher environmental prion loads in the future (Almberg et al., 2011), with the potential for



**TABLE 5** Comparison of remote sensing data sources for assessing animal aggregation

	Satellite	UAS	GPS
Spatial sample scale	Large area	Small area	Depends on areas used or co-used by collared animal
Temporal sample scale	One/day, most likely only 1 good image/3 days (weather dependent)	Up to several per day	Depends on fix interval, usually >1/day
Objective that best matches data source	Aggregation level at known maximum time matching satellite	Count of herd in targeted areas (e.g., winter range); maximum aggregation levels in areas with attractants (e.g., hay fields; feeding areas)	Evaluate drivers of movement and aggregation; identify locations with high site fidelity
Challenges	Weather; forest canopy; patchy snow or other conditions that camouflage elk; detection may be lower at low densities	Weather; forest canopy (thermal camera needed); airspace requirements; targeting far elk more difficult; targeted nature complicates comparisons	Getting large, distributed sample size
Time and Costs <sup>a</sup>	Time: Order, download, and evaluate image (2 h); pansharpen and orthorectify (1 h); digitize elk locations (8–16 h) COST: Depends on access.	Time: Travel; flight time (1 h); process (1 h); digitize elk locations (1–6 h) COST: UAS hardware, travel	Time: Collar deployment; collar processing COST: collars, capture expenses; more expensive

Abbreviations: UAS, unmanned aerial systems; GPS, Global Positioning System.

<sup>a</sup>Time estimates are averages per satellite image or UAS flight.

greater transmission of CWD that could result in significant population declines. CWD population modeling specific to the Jackson elk herd suggested that within 5 years of introduction, mean predicted CWD prevalence could reach 10%, and the population would decline at a 7% prevalence, even without cow elk harvest in the population (Galloway et al., 2017). CWD was detected in a hunter-killed elk nearby in Grand Teton National Park in fall 2020, ~2 years after a road-killed deer was detected in 2018.

Density estimates can be used to understand multiple aspects of habitat and space use across research and conservation applications. We provide insight on data sources and metrics to quantify animal aggregation. KDEs, KDE polygon area, and the first quantile of inter-elk distances provide the most valuable indices of the metrics considered here. Furthermore, kernel density contours can highlight areas of intensive use, which may be important for identifying areas of protection from disturbances, prioritizing locations of activities to reduce human–wildlife conflict, such as fencing or harvest, targeting collaring or other sampling programs, or optimizing soil or other treatments in areas where infectious agents for environmentally transmitted diseases may be concentrated. We expect the guidelines provided here

(Table 5) will assist others who are considering how to quantify animal density in open areas, for other density-dependent and environmentally transmitted diseases, at other winter ranges, and across a range of adaptive management options, including hunting, irrigation, fire, forestry, weed, or range treatments (Janousek et al., 2021). Following these guidelines, we conclude that GPS collars will provide the NER with the best information to evaluate how animal densities change with population size and planned changes in management, especially in spring when elk are more difficult to distinguish in satellite imagery with patchy snow cover.

**AUTHOR CONTRIBUTIONS**

Eric K. Cole, Geneva W.Chong, Aaron N. Johnston, Todd M. Preston, Tabitha A. Graves, and Paul C. Cross conceived the ideas. Eric K. Cole, Tabitha A. Graves, Aaron N. Johnston, and Todd M. Preston collected the data. Michael J. Yarnall, Tabitha A. Graves, Aaron N. Johnston, and Paul C. Cross designed analysis. Michael J. Yarnall, Tabitha A. Graves, Aaron N. Johnston, Todd M. Preston, and William M. Janousek analyzed the data. Tabitha A. Graves and Michael J. Yarnall led writing. All authors contributed critically to drafts and gave approval for publication.

## ACKNOWLEDGMENTS

Funding provided by the U.S. Fish and Wildlife Service, the U.S. Geological Survey Disease Program, and the U.S. Geological Survey North Central Climate Adaptation Science Center. The Grand Teton Association provided funding for GPS collars. Alyson Courtemanch provided Wyoming Game and Fish Department classification data. Sarah Gaulke assisted in preliminary analysis. Thanks to Dan Walsh and two anonymous reviewers. Any use of trade, firm, or product names is for descriptive purposes only and does not imply endorsement by the U.S. government.

## CONFLICT OF INTEREST

The authors declare no conflict of interest.

## DATA AVAILABILITY STATEMENT


Data (Graves et al., 2021) are available from the US Geological Survey ScienceBase repository at <https://doi.org/10.5066/P9GF8YYP>.


## ORCID

Tabitha A. Graves  <https://orcid.org/0000-0001-5145-2400>

Michael J. Yarnall 


Aaron N. Johnston  <https://orcid.org/0000-0003-4659-0504>

Todd M. Preston 

Geneva W. Chong 

Eric K. Cole 

William M. Janousek  <https://orcid.org/0000-0003-3978-1775>

Paul C. Cross 

## REFERENCES

- Almberg, E. S., P. C. Cross, C. J. Johnson, D. M. Heisey, and B. J. Richards. 2011. "Modeling Routes of Chronic Wasting Disease Transmission: Environmental Prion Persistence Promotes Deer Population Decline and Extinction." *PLoS One* 6(5): e19896. <https://doi.org/10.1371/journal.pone.0019896>.
- Anderson, C. B. 2018. "Biodiversity Monitoring, Earth Observations, and the Ecology of Scale." *Ecology Letters* 21: 1572–85. <https://doi.org/10.1111/ele.13106>.
- Baddeley, A., E. Rubak, and R. Turner. 2015. *Spatial Point Patterns: Methodology and Applications with R*. London: Chapman and Hall/CRC Press.
- Barasona, J. A., M. Mulero-Pázmány, P. Acevedo, J. J. Negro, M. J. Torres, C. Gortázar, and J. Vincente. 2014. "Unmanned Aircraft Systems for Studying Spatial Abundance of Ungulates: Relevance to Spatial Epidemiology." *PLoS One* 9(12): e115608. <https://doi.org/10.1371/journal.pone.0115608>.
- Becker, D. J., and R. J. Hall. 2014. "Too Much of a Good Thing: Resource Provisioning Alters Infectious Disease Dynamics in Wildlife." *Biological Letters* 10: 20140309. <https://doi.org/10.1098/rsbl.2014.0309>.
- Borchers, D. L., W. Zucchini, and R. M. Fewster. 1998. "Mark-Recapture Models for Line Transect Surveys." *Biometrics* 54: 1207–20.
- Bates, D., M. Mächler, B. M. Bolker, and S. C. Walker. 2015. "Fitting Linear Mixed-Effects Models Using lme4." *Journal of Statistical Software* 67: 1–48.
- Calenge, C. 2006. "The Package Adehabitat for the R Software: A Tool for the Analysis of Space and Habitat Use by Animals." *Ecological Modelling* 197: 516–9.
- Coe, P. K., D. A. Clark, R. M. Nielson, S. C. Gregory, J. B. Cupples, M. J. Hedrick, et al. 2018. "Multiscale Models of Habitat Use by Mule Deer in Winter." *Journal of Wildlife Management* 82: 1285–99. <https://doi.org/10.1002/jwmg.21484>
- Cross, P. C., J. Drewe, V. Patrek, G. Pearce, M. D. Samuel, and R. J. Delahay. 2009. "Wildlife Population Structure and Parasite Transmission: Implications for Disease Management." In *Management of Disease in Wild Mammals*, edited by R. J. Delahay, G. C. Smith, and M. R. Hutchings, 9–30. Tokyo: Springer.
- Cross, P. C., T. G. Creech, M. R. Ebinger, D. M. Heisey, K. Irvine, and S. Creel. 2012. "Wildlife Contact Analysis: Emerging Methods, Questions, and Challenges." *Behavioral Ecology and Sociobiology* 66: 1437–47. <https://doi.org/10.1007/s00265-012-1376-6>.
- Cross, P. C., W. H. Edwards, B. M. Scurlock, E. J. Maichak, and J. D. Rogerson. 2007. "Effects of Management and Climate on Elk Brucellosis in the Greater Yellowstone Ecosystem." *Ecological Applications* 17: 957–64. <https://doi.org/10.1890/06-1603>.
- Cross, P. C., T. G. Creech, M. R. Ebinger, K. Manlove, K. Irvine, J. Henningsen, J. Rogerson, B. M. Scurlock, and S. Creel. 2013. "Female Elk Contacts Are neither Frequency nor Density Dependent." *Ecology* 94: 2076–86. <https://doi.org/10.1890/12-2086.1>.
- Descamps, S., S. Jenouvrier, H. G. Gilchrist, and M. R. Forbes. 2012. "Avian Cholera, a Threat to the Viability of an Arctic Seabird Colony?" *PLoS One* 7: e29659. <https://doi.org/10.1371/journal.pone.0029659>
- Dorman, M. 2019. "nngeo: K-Nearest Neighbor Join for Spatial Data." R Package Version 0.2.9 <https://CRAN.R-project.org/package=nngeo>
- Dougherty, E. R., D. P. Seidel, C. J. Carlson, O. Spiegel, and W. M. Getz. 2018. "Going through the Motions: Incorporating Movement Analyses into Disease Research." *Ecology Letters* 21: 588–604. <https://doi.org/10.1111/ele.12917>.
- Fox, J., and S. Weisberg. 2011. *An R Companion to Applied Regression*, Second ed. Thousand Oaks, California, USA: Sage. <http://socserv.socsci.mcmaster.ca/jfox/Books/Companion>.
- Galloway, N. L., R. J. Monello, D. Brimeyer, E. K. Cole, and N. T. Hobbs. 2017. "Model Forecasting of the Impacts of Chronic Wasting Disease on the Jackson Elk Herd. 2017." United States Fish and Wildlife Service Technical Report.
- Gini, C. 1912, 1955. "Variabilità e mutabilità. Reprinted in" In *Memorie di metodologica statistica*, edited by E. Pizetti and T. Salvemini. Libreria Eredi Virgilio Veschi: Rome.
- Gini, C. 1921. "Measurement of Inequality of Incomes." *The Economic Journal* 31(121): 124–6. <https://doi.org/10.2307/2223319>.
- Gitzen, R. A., J. J. Millsaugh, and B. J. Kernohan. 2006. "Bandwidth Selection for Fixed-Kernel Analysis of Animal

- Utilization Distributions.” *Journal of Wildlife Management* 70(5): 1334–44. [https://doi.org/10.2193/0022-541X\(2006\)70\[1334:BSFFAO\]2.0.CO;2](https://doi.org/10.2193/0022-541X(2006)70[1334:BSFFAO]2.0.CO;2)
- Graves, T. A., M. J. Yarnall, A. J. Johnston, T. M. Preston, G. W. Chong, E. K. Cole, W. M. Janousek, and P. C. Cross. 2021. “Remotely Sensed Elk Locations on the National elk Refuge, Wyoming, 2018–2019.” U.S. Geological Survey Data Release <https://doi.org/10.5066/P9GF8YYP>.
- Hijmans, R. J. 2019. “raster: Geographic Data Analysis and Modeling.” R Package Version 3.0-2. <https://CRAN.R-project.org/package=raster>
- Hollings, T., M. Burgman, M. van Andel, M. Gilbert, T. Robinson, and A. Robinson. 2018. “How Do you Find the Green Sheep? A Critical Review of the Use of Remotely Sensed Imagery to Detect and Count Animals.” *Methods in Ecology and Evolution* 9: 881–92. <https://doi.org/10.1111/2041-210X.12973>.
- Janousek, W. M., T. A. Graves, G. Chong, E. K. Cole, E. Berman, and P. Cross. 2021. “Human Activities and Weather Drive Contact Rates of Wintering Elk.” *Journal of Applied Ecology* 58(3): 667–76. <https://doi.org/10.1111/1365-2664.13818>.
- Johnson, H. E., M. Hebblewhite, T. R. Stephenson, D. W. German, B. M. Pierce, and V. C. Bleich. 2013. “Evaluating Apparent Competition in Limiting the Recovery of an Endangered Ungulate.” *Oecologia* 171: 295–307. <https://doi.org/10.1007/s00442-012-2397-6>
- Kays, R., M. C. Crofoot, W. Jetz, and M. Wikelski. 2015. “Terrestrial Animal Tracking as an Eye on Life and Planet.” *Science* 348: aaa2478. <https://doi.org/10.1126/science.aaa2478>.
- Kendall, K., T. A. Graves, J. A. Royle, A. MacLeod, J. Boulanger, K. McKelvey, and J. Waller. 2019. “Using Bear Rub Data and Spatial Capture-Recapture Models to Estimate Trend in a Brown Bear Population.” *Scientific Reports* 9: 16804. <https://doi.org/10.1038/s41598-019-52783-5>.
- Kenward, M. G., and J. Roger. 1997. “Small Sample Inference for Fixed Effects from Restricted Maximum Likelihood.” *Biometrics* 53: 983–97.
- Kint, V., M. van Meirveene, L. Nachtergale, G. Geudens, and N. Lust. 2003. “Spatial Methods for Quantifying Forest Stand Structure Development: A Comparison between Nearest-Neighbor Indices and Variogram Analyses.” *Forest Science* 1: 36–49.
- LaRue, M. A., S. Stapleton, and M. Anderson. 2017. “Feasibility of Using High-Resolution Satellite Imagery to Assess Vertebrate Wildlife Populations.” *Conservation Biology* 31: 213–20. <https://doi.org/10.1111/cobi.12809>
- LaRue, M. A., S. S. Stapleton, C. C. Porter, T. Atwood, N. Lecomte, and S. Atkinson. 2015. “Testing Methods for Using High-Resolution Satellite Imagery to Monitor Polar Bear Abundance and Distribution.” *Wildlife Society Bulletin* 39: 772–9. <https://doi.org/10.1002/wsb.596>
- Lorenz, M. 1905. “Methods of Measuring the Concentration of Wealth.” *Publications of the American Statistical Association* 9(70): 209–19. <https://doi.org/10.2307/2276207>.
- Lloyd-Smith, J. O., P. C. Cross, C. J. Briggs, M. Daugherty, W. M. Getz, J. Latta, M. S. Sanchez, A. B. Smith, and A. Swei. 2005. “Should we Expect Population Thresholds for Wildlife Disease?” *Trends in Ecology & Evolution* 20(9): 511–9. <https://doi.org/10.1016/j.tree.2005.07.004>.
- McCallum, H., N. Barlow, and J. Hone. 2001. “How Should Pathogen Transmission Be Modelled?” *Trends in Ecology & Evolution* 16(6): 295–300. [https://doi.org/10.1016/S0169-5347\(01\)02144-9](https://doi.org/10.1016/S0169-5347(01)02144-9).
- Miguel, E., V. Grosbois, A. Caron, D. Pople, B. Roche, and C. A. Donnelly. 2020. “A Systematic Approach to Assess the Potential and Risks of Wildlife Culling for Infectious Disease Control.” *Communications Biology* 3: 353–67. <https://doi.org/10.1038/s42003-020-1032-z>.
- Mills, S. 2013. *Conservation of Wildlife Populations: Demography, Genetics, and Management*, Second ed. West Sussex, UK: John Wiley & Sons.
- Mikle, N. L., T. A. Graves, and E. M. Olexa. 2019. “To Forage or Flee: Lessons from an Elk Migration near a Protected Area.” *Ecosphere* 10(4): e02693. <https://doi.org/10.1002/ecs2.2693>.
- Monello, R. J., J. G. Powers, N. T. Hobbs, T. R. Spraker, M. K. Watry, T. L. Johnson, and M. A. Wild. 2014. “Survival and Population Growth of an Elk Population with a Long History of Exposure to Chronic Wasting Disease.” *Journal of Wildlife Management* 78: 214–23. <https://doi.org/10.1002/jwmg.665>
- National Land Cover Database. 2016. “Multi-Resolution Land Characteristics consortium.” <https://www.mrlc.gov/data/nlcd-2016-land-cover-conus>
- Pebesma, E. 2018. “Simple Features for R: Standardized Support for Spatial Vector Data.” *The R Journal* 10(1): 439–46. <https://doi.org/10.32614/RJ-2018-009>.
- Potapov, A., E. Merrill, M. Pybus, and M. A. Lewis. 2016. “Chronic Wasting Disease: Transmission Mechanisms and the Possibility of Harvest Management.” *PLoS One* 11(3): e0151039. <https://doi.org/10.1371/journal.pone.0151039>.
- Preston, T. M., M. L. Wildhaber, N. G. Green, J. L. Albers, and G. P. Debenedetto. 2021. “Enumerating White-Tailed Deer Using Unmanned Aerial Vehicles: A Case Study.” *Wildlife Society Bulletin* 45(1): 97–108. <https://doi.org/10.1002/wsb.1149>
- R Core Team. 2019. *R: A Language and Environment for Statistical Computing*. Vienna, Austria: R Foundation for Statistical Computing. <https://www.R-project.org/>.
- Ripley, B. D. 1977. “Modelling Spatial Patterns (with Discussion).” *Journal of the Royal Statistical Society, Series B* 39: 172–212.
- Ripley, B. D. 1988. *Statistical Inference for Spatial Processes*. Cambridge: Cambridge University Press.
- Rodríguez-Pastor, R., R. Escudero, D. Vidal, F. Mougeot, B. Arroyo, X. Lambin, et al. 2017. “Density-Dependent Prevalence of *Francisella tularensis* in Fluctuating Vole Populations, Northwestern Spain.” *Emerging Infectious Diseases* 23: 1377–9.
- Royle, J. A., R. Chandler, K. D. Gazenski, and T. A. Graves. 2013. “Spatial Capture-Recapture Models for Jointly Estimating Population Density and Landscape Connectivity.” *Ecology* 94: 287–94. <https://doi.org/10.1890/12-0413.1>
- Royle, J. A., R. B. Chandler, R. Sollmann, and B. Gardner. 2013. “Fully Spatial Capture-Recapture Models.” In *Spatial Capture-Recapture* 577. Waltham, MA: Academic Press.
- Sequeira, A. M. M., M. R. Heupel, M.-A. Lea, V. M. Eguiluz, C. M. Duarte, M. G. Meekan, M. Thums, et al. 2019. “The Importance of Sample Size in Marine Megafauna Tagging Studies.” *Ecological Applications* 29: e01947. <https://doi.org/10.1002/eap.1947>.
- Silverman, B. 1986. *Density Estimation for Statistics and Data Analysis*. London: Chapman and Hall.
- Smyser, T. J., R. J. Guenzel, C. N. Jacques, and E. O. Garton. 2016. “Double-Observer Evaluation of Pronghorn Aerial Line-Transsect Surveys.” *Wildlife Resources* 43: 474–81.

- Stapleton, S., M. LaRue, N. Lecomte, S. Atkinson, D. Garshelis, C. Porter, and T. Atwood. 2014. "Polar Bears from Space: Assessing Satellite Imagery as a Tool to Track Arctic Wildlife." *PLoS One* 9: e101513.
- Storm, D. J., M. D. Samuel, R. E. Rolley, P. Shelton, N. S. Keuler, B. J. Richards, and T. R. Van Deelen. 2013. "Deer Density and Disease Prevalence Influence Transmission of Chronic Wasting Disease in White-Tailed Deer." *Ecosphere* 4(1): 1–14. <https://doi.org/10.1890/ES12-00141.1>.
- Tosa, M. I., E. M. Schaubert, and C. K. Nielsen. 2015. "Familiarity Breeds Contempt: Combining Proximity Loggers and GPS Reveals Female White-Tailed Deer (*Odocoileus virginianus*) Avoiding Close Contact with Neighbors." *Journal of Wildlife Diseases* 51(1): 79–88. <https://doi.org/10.7589/2013-06-139>
- Tosa, M. I., E. M. Schaubert, and C. K. Nielsen. 2017. "Localized Removal Affects White-Tailed Deer Space Use and Contacts." *The Journal of Wildlife Management* 81(1): 26–37. <https://doi.org/10.1002/jwmg.21176>.
- Triguero-Ocaña, R., J. A. Barasona, F. Carro, R. C. Soriguer, J. Vicente, and P. Acevedo. 2019. "Spatiotemporal Trends in the Frequency of Interspecific Interactions between Domestic and Wild Ungulates from Mediterranean Spain." *PLoS One* 14(1): e0211216. <https://doi.org/10.1371/journal.pone.0211216>.
- U.S. Fish and Wildlife Service and National Park Service, U.S. Department of the Interior. 2007. "Final Bison and Elk Management Plan and Environmental Impact Statement, National Elk Refuge, Grand Teton National Park, and John D. Rockefeller, Jr., Memorial Parkway." Denver, CO.
- U.S. Fish and Wildlife Service. 2019. "Bison and Elk Management Step-down Plan. National Elk Refuge, Grand Teton National Park, Wyoming." Lakewood, CO: U.S. Department of the Interior, U.S. Fish and Wildlife Service. National Park Service.
- Venesky, M. D., J. L. Kerby, A. Storfer, and M. J. Parris. 2011. "Can Differences in Host Behavior Drive Patterns of Disease Prevalence in Tadpoles?" *PLoS One* 6: e24991.
- Wang, D., Q. Shao, and H. Yue. 2019. "Surveying Wild Animals from Satellites, Manned Aircraft and Unmanned Aerial Systems (UASs): A Review." *Remote Sensing* 11: 1308.
- Wilschut, L., A. Laudisoit, N. K. Hughes, E. A. Addink, S. M. de Jong, A. P. Heesterbeek, et al. 2015. "Spatial Distribution Patterns of Plague Hosts: Point Pattern Analysis of the Burrows of Great Gerbils in Kazakhstan." *Journal of Biogeography* 42(7): 1281–92. <https://doi.org/10.1111/jbi.12534>.
- Witczuk, J., S. Pagacz, A. Zmarz, and M. Cypel. 2017. "Exploring the Feasibility of Unmanned Aerial Vehicles and Thermal Imaging for Ungulate Surveys in Forests - Preliminary Results." *International Journal of Remote Sensing* 39: 1–18.
- Worton, B. 1989. "Kernel Methods for Estimating the Utilization Distribution Inhome-Range Studies." *Ecology* 70: 164–8.
- Xue, Y., T. Wang, and A. K. Skidmore. 2017. "Automatic Counting of Large Mammals from Very High Resolution Panchromatic Satellite Imagery." *Remote Sensing* 9: 878.
- Yang, Z., T. Wang, A. K. Skidmore, L. J. De, M. Y. Said, and J. Freer. 2014. "Spotting East African Mammals in Open Savanah from Space." *PLoS One* 9: e115989.

## SUPPORTING INFORMATION

Additional supporting information may be found in the online version of the article at the publisher's website.

**How to cite this article:** Graves, Tabitha A., Michael J. Yarnall, Aaron N. Johnston, Todd M. Preston, Geneva W. Chong, Eric K. Cole, William M. Janousek, and Paul C. Cross. 2022. "Eyes on the Herd: Quantifying Ungulate Density from Satellite, Unmanned Aerial Systems, and GPScollar Data." *Ecological Applications* 32(5): e2600. <https://doi.org/10.1002/eap.2600>